Received: 18 January 2024 | Revised: 25 March 2024 | Accepted: 30 March 2024

DOI: 10.1002/ppap.202400018

RESEARCH ARTICLE

PLASMA PROCESSES AND POLYMERS

Stretch-tolerant PECVD gas barrier coatings for sustainable flexible packaging

Philipp Alizadeh | **Jonas Franke** | **Rainer Dahlmann**

Institute for Plastics Processing (IKV) in Industry and Craft at RWTH Aachen University, Aachen, Germany

Correspondence
Philipp Alizadeh, Institute for Plastics Processing (IKV) in Industry and Craft at RWTH Aachen University, 502047 Aachen, Germany.
Email: Philipp.Alizadeh@ikv.rwth-aachen.de

Funding information
Deutsche Forschungsgemeinschaft

Abstract

This study employs X-ray photoelectron spectroscopy (XPS), thickness measurements, permeation analysis and laser scanning microscopy to analyse the stretch tolerance in dependence of the chemical composition and deposition rates of plasma-enhanced chemical vapour deposition coatings. SiO_x and SiOCH coatings are deposited on polyethylene terephthalate film using a full factorial study design of three parameters (monomer/oxygen mass flow and pulse duration). They exhibit distinct differences, with the monomer mass flow emerging as a critical factor influencing deposition rates and stretch tolerance. SiOCH coatings demonstrate faster growth rates due to higher monomer flow. SiO_x coatings exhibit superior barrier performance. Stretch tolerance does not solely correlate with atomic composition, since a SiO_x coating with higher-than-predicted stretch tolerance was observed.

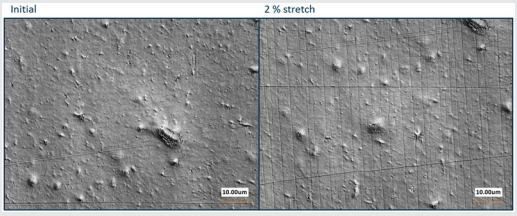

KEYWORDS
oxygen transmission rate, plasma enhanced chemical vapour deposition, silicon oxide film, single layer barrier, stretch tolerance

1 | INTRODUCTION

Flexible packaging must provide high-level product protection within complex supply chains. Requirements for mechanical integrity, flexibility, barrier properties against gases and cost-effective production must be met simultaneously. For instance, in food packaging, plastics play a crucial role in extending the shelf life of food, thereby reducing food waste.

Among recyclable materials, thermoplastics offer significant potential for mechanical recycling, but achieving effective separation by material type necessitates mono-material solutions. The low gas barrier function of many thermoplastics however limits their applicability. Packaging solutions made of multimaterial composites are therefore commonly used. Layers composed of various plastics, metallised layer or paper are combined to meet the diverse demands.

Abbreviations: HMDSO, hexamethyldisiloxane; LSM, laser scanning microscopy; PECVD, plasma-enhanced chemical vapour deposition; PET, polyethylene terephthalate; XPS, X-ray photoelectron spectroscopy.

One approach to functionalising plastic films without compromising their recyclability is obtained by applying plasma-enhanced chemical vapour deposition (PECVD).[1] This process, conducted in technical low-pressure plasmas, maintains a temperature close to ambient levels due to the extended mean free path length in the vacuum, regardless of the gas mixture ratio.[2] This allows for the coating of thermally sensitive materials.

One of the key issues in coating flexible web material for packaging applications is convertibility. Plastic films undergo numerous rewinding operations during processing into packaging and are subjected to a wide variety of mechanical stresses during handling. Numerous research groups have studied the performance of PECVD barrier coating systems under mechanical loading, focusing in particular on tensile and bending loads[3–9] The main coating systems investigated include SiO_x[3,6,8,10] and AlO_x[7,9] coatings, which are widely used in the packaging market, but also in areas such as the semiconductor industry.[10,11]

Defects are caused by induced stresses when the coatings are deformed, whereby tensile stresses have been identified as particularly damaging.[11] Therefore, a number of studies are pursuing an approach in which composite materials are created.[3,7,10,11] This can be achieved by a multilayer architecture of nanolayers as well as by the joining of multiple coated plastic films. Through different stiffness values, stresses can be absorbed by surrounding material layers and thus mechanically relieve barrier coatings.

Within the nanoscopic coating architecture, however, it is also possible to influence the mechanical load capacity of the coatings by influencing their intrinsic stress states. For example, by combining different chemical compositions of layer systems, bending tolerance and thus the underlying stress absorption can be improved. This can be achieved, for example, by a combination of AlO_x and SiO_x, but in the case of hexamethyldisiloxane (HMDSO) also with the help of only one monomer. In this case, both organosilicon and silicon oxide layers are deposited in a multilayer system, each of which generates opposite intrinsic stresses.[10,12]

Another decisive coating property that influences the mechanical load-bearing capacity of the barrier film is the coating thickness. Especially for Al_2O_3 coatings, it could be shown that the strain and bending tolerance of the coatings increases significantly with decreasing coating thickness.[13,14] In a multilayer architecture consisting of indium zinc oxide, SiO_x and AlO_x as an intermediate layer, the same could be observed for the reduction of the SiO_x layer thickness from 300 to 90 nm. From this, it can be deduced that coating systems must be produced particularly free of defects to guarantee high barrier performances at low coating thicknesses. In terms of convertibility, several studies can be found with satisfactory bending tolerances, which are in the range of 20–40 mm bending radius.[3,10,13]

In the development of plasma–polymer silicon coatings, the coating parameters can be used to adjust the coating chemistry and thus properties such as the barrier effect or the intrinsic stresses or the strain tolerance over a wide range.[15–18] With regard to strain-tolerant barrier coatings, a conflict of objectives seems to arise, as the coating chemistry can be varied on a spectrum between strongly organosilicon (SiOCH) compounds to strongly inorganic SiO_x compounds. The SiO_x compounds are brittle like glass and have a good barrier effect against gases. The SiOCH compounds, on the other hand, are stretchable but have hardly any barrier effect against gases.[19] Multiple investigations have been conducted that focus on the coating architecture. For example, multilayer coatings consisting of SiOCH and SiO_x coatings or the coating of both sides of a plastic film can be applied to improve strain tolerance.[19–21]

2 | EXPERIMENTAL SECTION

2.1 | Materials

The chosen film substrate for all experiments was a biaxially orientated polyethylene terephthalate (PET) with a thickness of 12 μm by Flex Films Inc. The used monomer was HMDSO with a purity of 98.5% by Merck KGaA. The oxygen gas used for synthesis and permeation measurements as well as the nitrogen gas used as a carrier for permeation measurements had a purity of at least 99.999% (both gases supplied by Westfalen AG). For the determination of coating thicknesses polished Si wafers by Si-Mat were used.

2.2 | Coating reactor and parameters

All coatings were deposited in the custom-designed PECVD reactor for large-area flat substrates. The reactor uses a remote plasma configuration, where four plasma lines with a respective power of 4 kW emit microwave radiation at a frequency of 2.45 GHz. The reactor has a substrate holder measuring 300 mm × 300 mm. A transfer system with dimensions of approximately 75 mm × 100 mm was used for the coating tests to ensure faster

sample changes and less contamination of the vacuum. The samples for the conventional tensile test and for the microtensile test were coated simultaneously in the same process. The homogeneity of the coating deposition was analysed in detail for the entire substrate holder with regard to coating thickness, coating stress, coating chemistry and coating barrier properties and improved.[22] The already improved homogeneity is additionally controlled by the limited area of the transfer system used.

The microwave power is introduced in a pulsed mode. A square wave signal with a defined pulse duration and pulse pause is generated for this purpose. The full power is applied during the pulse duration. No power is applied during the pulse pause (see Table 1).

Further descriptions of duo plasma lines and the utilised reactor are found elsewhere.[23–25] To contribute to a deeper understanding of the role of the process parameters in the deposition of stretch-tolerant SiO_x and SiOCH coatings, a variation of the monomer and oxygen mass flow as well as the pulse duration was performed. A full-factorial experimental design with two parameter levels was pursued to evaluate the significance for each of the parameter's monomer and oxygen mass flow as well as pulse duration separately. The process parameters are based on earlier studies on the same reactor.[12,17] The eight resulting parameter sets were obtained by variations of the process gas mass flows and pulse durations in two levels, respectively. They can be obtained from Table 1. Monomer concentrations in the process gas vary from 3.85% to 16.67%

The process pressure was constantly regulated to 5 Pa with the aid of a butterfly valve. All process steps were preceded by a 20 s purge time. The fed-in power was 4 kW per plasma line for all process steps in this study.

2.3 | Analysis instruments

The chemical compositions of the coating layers were carried out using an X-ray photoelectron spectroscopy (XPS) (M-probe; Surface Science). Chemical composition of the coatings was calculated from the characteristic peak intensity ratio. Monochromatised Al Kα radiation at 1486.6 eV, a pass energy of 217.36 eV for survey spectra and 84.02 eV for core level peaks were used for the analysis. The pressure during the measurements was less than 2×10^{-8} mbar. We analysed a survey spectrum as well as the C 1s, O 1s and Si 2p core peaks. In each measurement, an elliptical measurement area with a size of 750 μm^2 was evaluated. The angle between electron analyser and sample surface was 55°. To avoid electrical charging of the sample surface, a low-energy electron beam (5 eV) was used during measurements. The CasaXPS analysis software from Casa Software Ltd. was used to evaluate measurement results. The C 1s peak was always set to 285 eV (carbon peak) to make the measurement results comparable.

TABLE 1 Process parameters.

	1: Gas flow		2: Duty cycle		
	Precursor	Auxiliary gas	Pulse duration	Pulse pause	3: Coating time
Name	HMDSO (sccm)	O_2 (sccm)	t_{on} (ms)	t_{off} (ms)	$t_{coating}$ (s)
Pretreatment	0	100	4	40	5
P0,A0,T0	10	150	3	45	40 + 60[a]
P1,A0,T0	30				
P0,A1,T0	10	250			
P1,A1,T0	30				
P0,A0,T1	10	150	4		
P1,A0,T1	30				
P0,A1,T1	10	250			
P1,A1,T1	30				

Abbreviation: HMDSO, hexamethyldisiloxane.

[a]Thickness values were estimated for two coated samples depending on coating times (40 and 60 s) for all test points. For further information, see Section 3.2.

Coating thickness measurements were conducted by stylus profilometry using Alpha-Step® D-600 Stylus Profiler by KLA-Tencor.

To determine the oxygen transmission rates (OTRs) of the investigated PET film substrates as well as of deposited coatings, oxygen permeation was measured using the carrier gas with an M8001 by Systech Instruments Ltd. As testing gas dry oxygen was used and dry nitrogen was used as carrier gas.

Microscopy analysis was conducted using a laser scanning microscope (LSM) (VK-X200; Keyence).

Crack densities were obtained by the complementary use of LSM and a microtensile-compression module (Kammrath & Weiss GmbH). Coated films were subjected to a step-wise elongation of up to 10% in 1% intervals.

Additional analysis of the stretch tolerance was conducted by measuring the OTR as a direct response to a defined elongation. Therefore, four samples per test point were coated and elongated to 1%. The preload was set to 5 N and the testing velocity to 5 mm min^{-1}. The distance between the clamping blocks was 81 mm at the start of all test runs.

3 | RESULTS AND DISCUSSION

3.1 | Chemical analysis by means of XPS

A comprehensive overview of the chemical analysis by means of XPS for all sample types is given in Figure 1. The atomic composition is visualised as a percentage while the columns represent the respective ratios of carbon-to-silicon (C/Si), oxygen-to-silicon (O/Si) and carbon-to-oxygen (C/O). While the silicon content remained nearly constant, significant changes in oxygen and carbon content are observable. The samples can be divided into two groups. The even sample numbers appear to be more organic SiOCH coatings in general. The odd sample numbers on the other hand appear to be rather inorganic SiO_x coatings.

The main distinguishing factor between the two groups is the precursor mass flow, which ranges from 10 sccm for the SiO_x coatings to 30 sccm for the SiOCH coatings. An increase in the oxygen mass flow leads to a slight increase in the oxygen content of the coatings. This effect is less pronounced than the influence of the monomer mass flow. In general, the oxygen/silicon ratio is slightly lower for 4 ms pulse duration than for shorter pulse duration of 3 ms. This observation is contrary to expectation since higher energy densities correlate with a higher oxygen content for an oxygen-rich process gas mixture. Due to the greater degree of fragmentation, the probability of oxygen ions substituting carbon atoms in the coating structure is increased.[17]

3.2 | Investigation of the deposition rates

The deposition rates shown in Figure 2a confirm the distinction between SiO_x and SiOCH coatings with deposition rates significantly higher for SiOCH coatings than for SiO_x coatings. All coatings were applied on polished silicon wafers. For each coating, two wafers were coated for 40 and 60 s, respectively. Four measurements of the coating thickness were conducted for each wafer. The mean deposition rate after both coating times was then derived under the assumption of a linear coating growth.

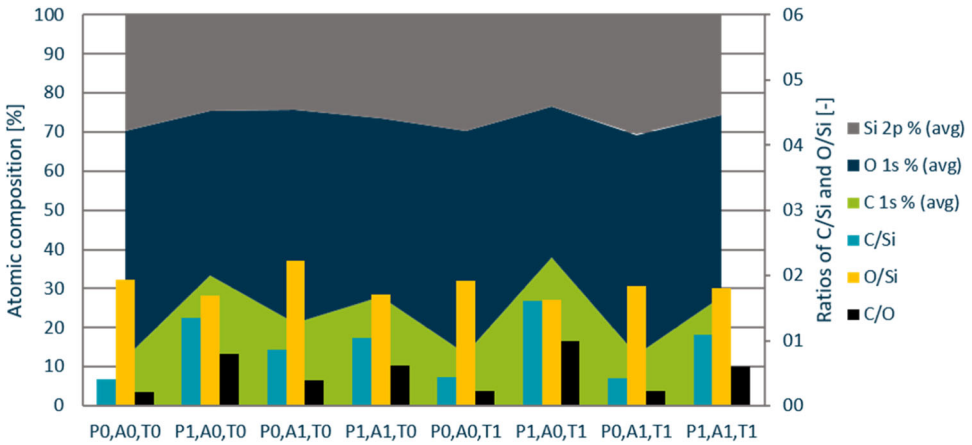

FIGURE 1 Overview of the respective atomic compositions as well as selected element ratios obtained by X-ray photoelectron spectroscopy.

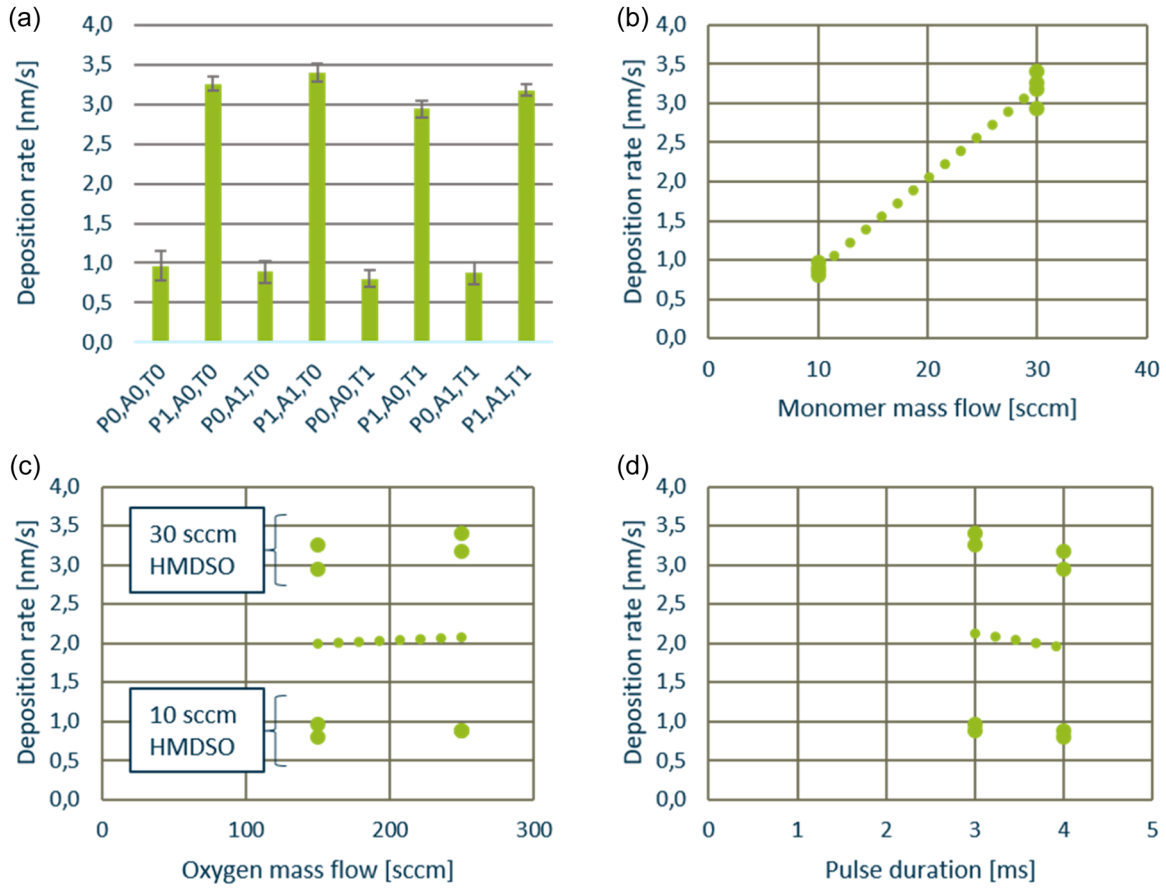

FIGURE 2 Deposition rates for each coating (a) and depending on the process parameters precursor mass flow (b), oxygen mass flow (c), and pulse duration (d).

An approximately three times higher deposition rate was observed for the SiOCH coatings, which is consistent with earlier studies from the literature.[17] The higher mass flow of HMDSO directly caused a faster coating growth. For the SiOCH coatings, a higher concentration of HMDSO in the process gas mixture makes volume polymerisation more likely and thus leads to a faster deposition and more granular coating structures. For lower concentrations of precursor, the oxygen mass flow suppresses the volume polymerisation and promotes the incorporation of oxygen into the coating structure, which leads to lower deposition rates.[12]

A comprehensive overview of the influences of the process parameters on the coating deposition rate is given in Figure 2b–d. It is striking that the precursor mass flow is the most influential process parameter, while oxygen mass flow and pulse duration are only slightly affecting the deposition rate. Hegemann has presented a subdivision of coating states in which the process can be divided into an energy-deficient and a monomer-deficient regime. The coating deposition rate can therefore be limited by either the prevailing energy density and the available monomer.[26]

Since the strongest interaction between deposition rate and monomer mass flow is observable, all conducted experimental points are in the monomer-deficient regime. Therefore, the slight increase of the deposition rate as a consequence of increasing the oxygen mass flow (Figure 2c) occurs despite the resulting reduction in energy density, in such a way that additional available oxygen can be incorporated into the coating system. For an increase in pulse duration, with otherwise constant parameters, a slight reduction in the deposition rate is observed. Consequently, an increase in energy density leads to a slight decrease in the deposition rate.

Possible explanatory hypotheses could be based on the assumption that, for a given process gas composition, an increase in energy density leads to a coating with a higher degree of cross-linking. For example, effects such as ion peening can lead to a densification of the coating as a result of bombardment with higher energy ions.[27]

3.3 | Assessment of the strain tolerance

Strain tolerance is defined as the ability of a coating to undergo mechanical stress without an impairment of its functionality. In the following section, the strain tolerance of the investigated coatings is discussed based on analyses regarding their OTR as well as the onset of crack formation under defined elongation.

3.3.1 | OTR

The initial barrier performance before the coated films were subjected to stretching was first analysed. Figure 3 shows the OTR value of the test points in the form of columns. For each value, four PET samples were coated for a target thickness of 30 nm and measured. Coating times were derived by the deposition rates obtained from Section 3.2.

The clear differentiation between SiO_x and SiOCH from the previous investigations continues in these values, so that the SiO_x layers deliver significantly better barrier performance and therefore distinctively lower OTR values than the SiOCH layers.

The respective process parameters of the test points are represented by the graphs. Once again, the monomer mass flow is the strongest influencing parameter. A statistical analysis confirms the significance with a p value of approximately 0.009. This corresponds to an error probability of approximately 0.9% that the effect of the monomer mass flow parameter does not occur by chance.

The parameter's oxygen mass flow and pulse duration have significantly weaker effects, which must be taken into account in the interpretation. It is noticeable, however, that an increase in the pulse duration (P0,A0,T0–P1,A1,T1) leads to a slight increase in the OTR values for all test points. This is consistent with the XPS analysis, which shows an increased carbon content for these same test points (Figure 1). Interestingly, in a direct comparison of test points P0,A0,T1 and P1,A0,T1 with test points P0,A1,T1 and P1,A1,T1, an increase in oxygen mass flow leads to slightly poorer barrier performance despite the higher oxygen content. The lowest OTR value is achieved for test point P0,A1,T0 (low monomer concentration and low pulse duration) and the highest for test point P1,A1,T1 (medium monomer concentration and high pulse duration).

The respective OTR values before and after elongation are visualised in Figure 4. The OTR value of the uncoated films ($154 \pm 4\ cm^3\ day^{-1}\ m^{-2}\ bar^{-1}$) is given for reference. Contrary to the initial hypothesis, there is no consistent observable distinction between the stretch tolerances of SiO_x and SiOCH coatings in general. Both types of coatings have more and less stretch-tolerant test points in the framework of the investigation. Test points P0,A1,T1 and P1,A1,T1 show lower OTR mean values for the stretched samples. Due to the high standard deviations, it is conceivable that the real OTR remains unchanged by the elongation. The same assumption can be made for P0,A0,T0 despite the fact that the elongated mean OTR is slightly higher than the non-stretched mean OTR.

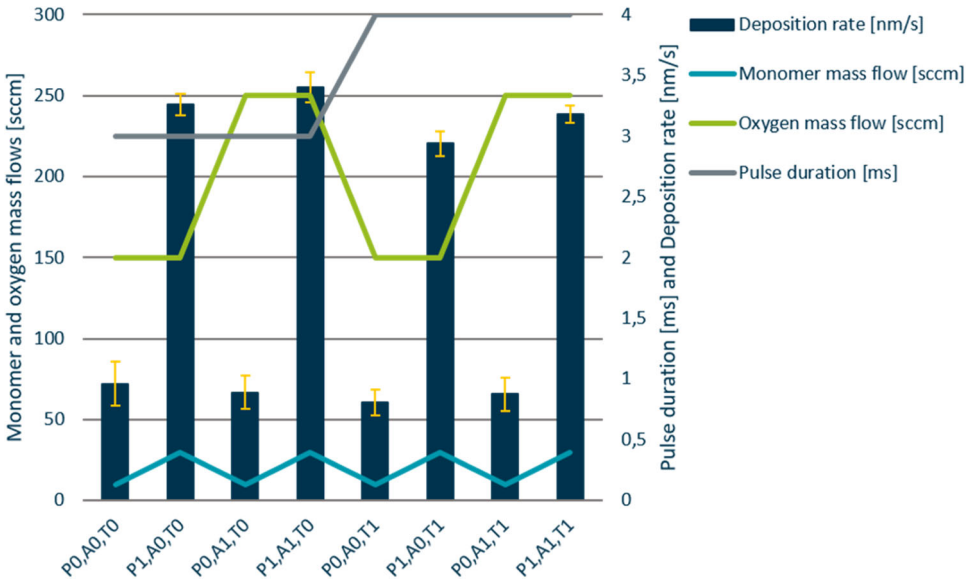

FIGURE 3 Overview of the initial oxygen transmission rate before stretching and underlying process parameters for each coating.

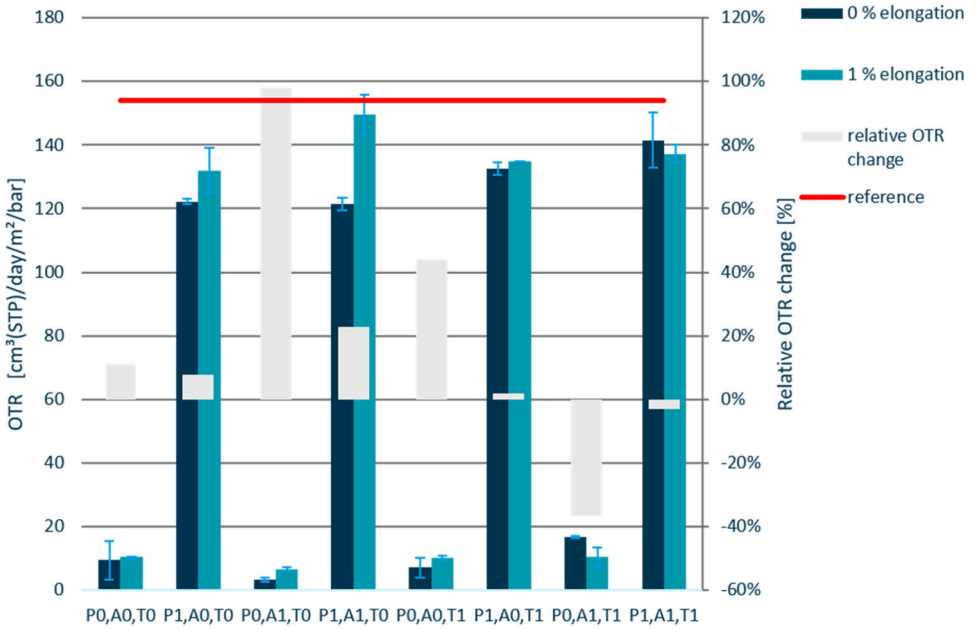

FIGURE 4 Respective oxygen transmission rate values before and after stretching for each coating.

3.3.2 | Crack formation

Since higher elongation values are relevant in the context of an application of SiO_x coatings in the packaging sector, a broader investigation of the stretch tolerance was conducted by means of LSM. During the tests, the coated films were subjected to a step-wise elongation of up to 10% with the help of a microtensile test module, whereby the measurement was divided into 1% intervals. The resolution of LSM is in the micrometre range and the coating systems have thicknesses in the low two-digit nanometre range. Since nanoscopic cracks can occur at much lower elongations than microscopic cracks, the lower resolution has to be taken into account during interpretation.

An overview of the detection of the onset of crack formation for all coating systems is given in Figure 5a.

The onset of crack formation varies from 1% (P0,A1,T0) to 7% (P1,A0,T0). On average the SiO_x coatings tend to form cracks at lower elongation values than the SiOCH coatings. The picture is completed when considering the oxygen mass flow, as generally higher elongation tolerances can be observed at 150 sccm than at 250 sccm. Oxygen flow is directly related to the carbon/oxygen ratio of the coatings, meaning that a higher elongation tolerance can generally be observed for more organic coatings. However, this effect is much less pronounced than the influence of the monomer mass flow. The pulse duration shows a slight tendency for lower strain tolerance at higher pulse durations. However, these general trends are not confirmed, particularly in the case of coatings P0,A0,T0 and P1,A1,T1. Here, P0,A0,T0 is above the expected value while P1,A1,T1 is below.

If the chemical composition of the coatings is compared to the crack formation elongation, a general trend can be seen that shows an increasing elongation at onset of crack formation with increasing carbon/oxygen ratio (Figure 6). Broadly viewed, an approximately linear relationship between these variables can be assumed in the context of the study.

Despite this general trend, the linear approximation is surrounded by outliers. Coating P0,A0,T0 is an outlier towards a higher-than-expected elongation tolerance. Coatings P0,A0,T1 and P0,A1,T1 have a carbon/oxygen ratio of approximately 0.2 and show crack formation from an elongation of 2%. Coating P0,A0,T0, on the other hand, only shows crack formation at 4% elongation with a similar carbon/oxygen ratio. It is striking that the clear distinction of SiO_x and SiOCH coatings cannot be observed for this test, despite the fundamental differences in coating chemistry. Instead, a very distinct stretch tolerance is observed for coatings with similar chemical compositions.

To achieve a deeper understanding of those phenomena the crack density per 10 μm was derived for each step of the stretch experiment. From Figure 7, the crack density for each coating and step of the experiment can be obtained.

While a closer correlation between atomic composition and strain tolerance can still be observed when analysing the onset of crack formation, a comparison of

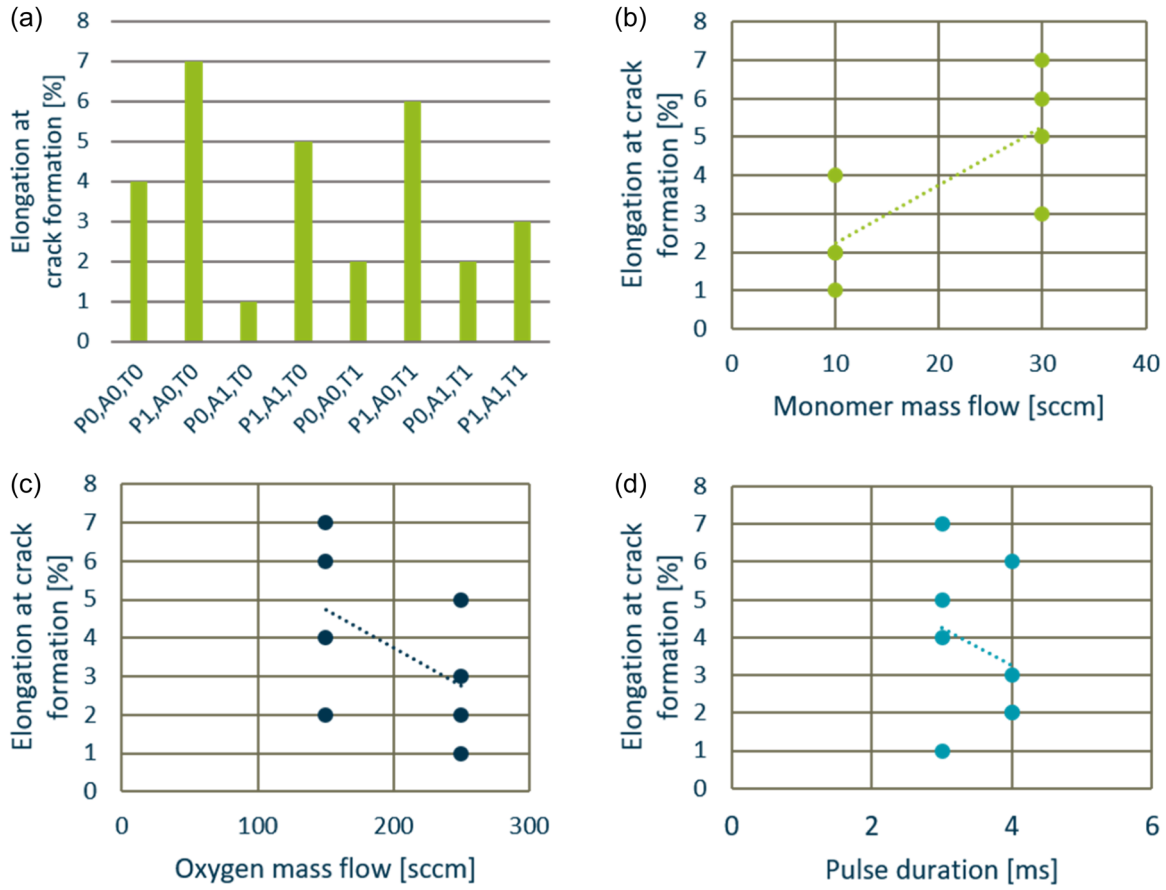

FIGURE 5 Respective elongation values at the onset of crack formation for each coating (a) and respective dependence of the process parameters monomer mass flow (b), oxygen mass flow (c), and pulse duration d).

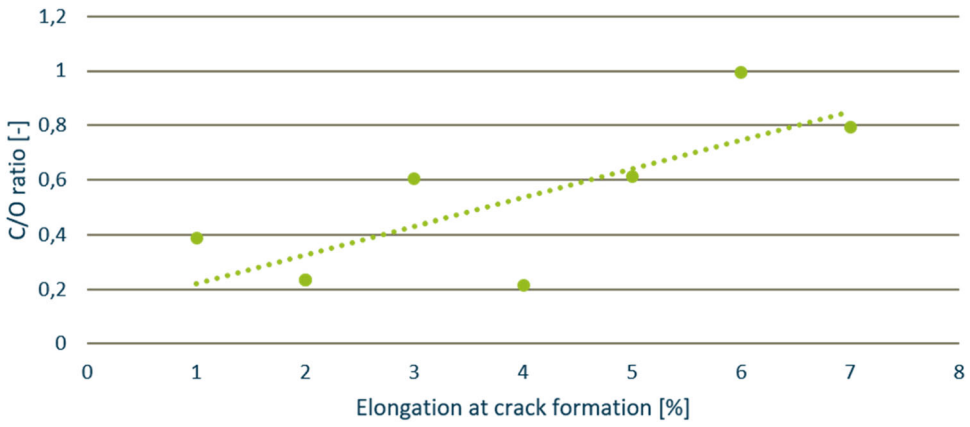

FIGURE 6 Elongation at the onset of crack formation as a function of the carbon-to-oxygen ratio.

the crack densities at higher strain values no longer shows a clear correlation with the atomic composition. It is striking that for P0,A0,T0 not only an offset beginning of crack formation compared to expectation is observed but also the lowest crack density at elongation values of 8%–10%. Looking at the atomic composition of coatings P0,A0,T0, P0,A0,T1 and P0,A1,T1, no distinct differences can be observed (Figure 1), which raises the question, which other fundamental coating properties besides the atomic composition determine stretch tolerance. Another striking detail is the rapid increase of crack density observed for coating P0,A1,T0. It appears to be the most inorganic coating with the highest O/Si ratio of 2.2 in the framework of the investigation (Figure 1).

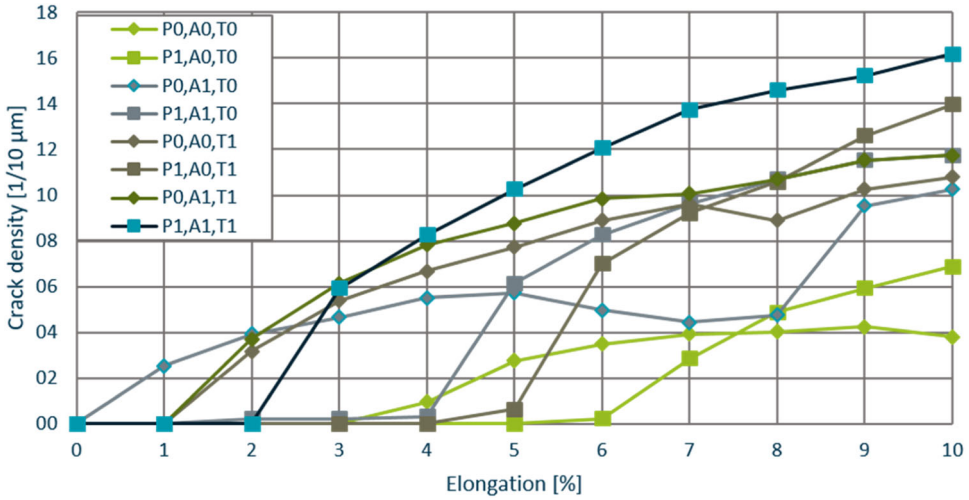

FIGURE 7 Standardised crack density as a function of the elongation.

Therefore, it is conceivable that the chemical structure is mostly glass-like and brittle. The initial OTR value before stretching is also in accordance with this observation, since it is the lowest in the framework of this investigation.

4 | CONCLUSION

The comprehensive investigation into strain-tolerant PECVD coatings utilising XPS, OTR analysis and LSM investigation has yielded valuable insights. The key findings include distinct differences between SiO_x and SiOCH coatings, with the monomer mass flow emerging as a crucial factor influencing deposition rates and stretch tolerance. SiOCH coatings, characterised by higher monomer flow, exhibit faster growth rates, while SiOx coatings demonstrate superior barrier performance and tend to form cracks at lower elongation values in general. Despite this trend, there are outliers that do not exhibit this behaviour under strain, but instead show a comparatively medium to high stretch tolerance while at the same time providing barrier function and a rather inorganic chemical composition.

Interestingly, the stretch tolerance of these coatings does not solely correlate with atomic composition, as evidenced by the crack density analysis at higher strain values as well as the analyses of the elongation at the onset of crack formation. This suggests the involvement of additional fundamental coating properties in determining stretch tolerance. Further research is needed to understand these phenomena comprehensively.

Possible causes for the observed behaviour could include additional coating properties such as the degree of cross-linking, the surface morphology and the internal structure. Therefore, the investigation of the surface structure using atomic force microscopy or the investigation of the nanostructure using transmission electron microscopy could provide crucial information.

To generate further information about the strain tolerance in connection with permeation, coating systems should be subjected to further OTR measurements after stretch experiments with higher elongation values. In addition, subsequent investigations with multilayer systems could significantly improve the strain tolerance by decoupling the stress states of the SiO_x layers with SiOCH layers.

ACKNOWLEDGEMENTS

Some of the work shown in this article received support from the German Research Foundation (DFG) within the framework of the Transregional Collaborative Research Centre TRR 87/1 (SFB-TR 87) "Pulsed High Power Plasmas for the Synthesis of Nanostructural Functional Layers." We would like to thank the DFG. Open Access funding enabled and organized by Projekt DEAL.

CONFLICT OF INTEREST STATEMENT

The authors declare no conflict of interest.

DATA AVAILABILITY STATEMENT

The data that support the findings of this study are available from the corresponding author upon reasonable request.

ORCID

Philipp Alizadeh http://orcid.org/0000-0002-4581-7618

REFERENCES

[1] H. Yasuda, Y. Matsuzawa, *Plasma Process. Polym.* **2005**, *2*, 507.
[2] D. Binkowski, *Plasmapolymere Barriereschichten für Kunststoffe: Verfahren, Materialien und Eigenschaften*, RWTH, Aachen **2008**.
[3] Z. Liu, Z. Sun, X. Ma, C. L. Yang, *Packag. Technol. Sci.* **2013**, *26*, 70.
[4] J. Andersons, Y. Leterrier, I. Fescenko, *Thin Solid Films* **2003**, *434*, 203.
[5] L. Han, P. Mandlik, J. Gartside, S. Wagner, J. A. Silvernail, R.-Q. Ma, M. Hack, J. J. Brown, *J. Electrochem. Soc.* **2009**, *156*, H106.
[6] M. Yanaka, B. M. Henry, A. P. Roberts, C. R. M. Grovenor, G. A. D. Briggs, A. P. Sutton, T. Miyamoto, Y. Tsukahara, N. Takeda, R. J. Chater, *Thin Solid Films* **2001**, *397*, 176.
[7] A. Parhi, J. Tang, S. S. Sablani, *Food Packag. Shelf Life* **2020**, *25*, 100514.
[8] M. V. Tavares da Costa, E. K. Gamstedt, *Surf. Coat. Technol.* **2021**, *426*, 127746.
[9] R. L. Kovács, S. Gyöngyösi, G. Langer, E. Baradács, L. Daróczi, P. Barkóczy, Z. Erdélyi, *Thin Solid Films* **2021**, *738*, 138960.
[10] G.-H. Lee, J. Yun, S. Lee, Y. Jeong, J.-H. Jung, S.-H. Cho, *Thin Solid Films* **2010**, *518*, 3075.
[11] N. Kim, S. Graham, *Thin Solid Films* **2013**, *547*, 57.
[12] M. Jaritz, C. Hopmann, S. Wilski, L. Kleines, L. Banko, D. Grochla, A. Ludwig, R. Dahlmann, *J. Phys. D***2020**, *53*, 345203.
[13] S.-H. Jen, J. A. Bertrand, S. M. George, *J. Appl. Phys.* **2011**, *109*, 084305. https://doi.org/10.1063/1.3567912
[14] Y. Zhang, R. Yang, S. M. George, Y.-C. Lee, *Thin Solid Films* **2011**, *520*, 251.
[15] M. Jaritz, C. Hopmann, S. Wilski, L. Kleines, M. Rudolph, P. Awakowicz, R. Dahlmann, *Surf. Coat. Technol.* **2019**, *374*, 232.
[16] M. Jaritz, C. Hopmann, S. Wilski, L. Kleines, M. Rudolph, P. Awakowicz, R. Dahlmann, *J. Mater. Eng. Perform.* **2020**, *29*, 2839.
[17] M. Jaritz, P. Alizadeh, S. Wilski, L. Kleines, R. Dahlmann, *Plasma Process. Polym.* **2021**, *18*, e2100018. https://doi.org/10.1002/ppap.202100018
[18] P. Alizadeh, S. Wilski, R. Dahlmann, *Prog. Org. Coat.* **2022**, *172*, 107064.
[19] K. Bahroun, H. Behm, C. Hopmann, R. Dahlmann, S. Wald, K. Vissing, *J. Oberflächentec.***2014**, *54*, 34.
[20] E. Schmachtenberg, F. R. Costa, S. Göbel, *J. Appl. Polym. Sci.* **2005**, *99*, 1485.
[21] K. Bahroun, *Dissertation*, RWTH Aachen University (Aachen) **2017**.
[22] D. Kirchheim, S. Wilski, M. Jaritz, F. Mitschker, M. Oberberg, J. Trieschmann, L. Banko, M. Brochhagen, R. Schreckenberg, C. Hopmann, M. Böke, J. Benedikt, T. de los Arcos, G. Grundmeier, D. Grochla, A. Ludwig, T. Mussenbrock, R. P. Brinkmann, P. Awakowicz, R. Dahlmann, *J. Coat. Technol. Res.* **2019**, *16*, 573.
[23] K. Bahroun, H. Behm, F. Mitschker, P. Awakowicz, R. Dahlmann, C. Hopmann, *J. Phys. D***2014**, *47*, 015201.
[24] W. Petasch, E. Räuchle, H. Muegge, K. Muegge, *Surf. Coat. Technol.* **1997**, *93*, 112.
[25] M. Jaritz, C. Hopmann, H. Behm, D. Kirchheim, S. Wilski, D. Grochla, L. Banko, A. Ludwig, M. Böke, J. Winter, H. Bahre, R. Dahlmann, *J. Phys. D***2017**, *50*, 445301.
[26] D. Hegemann, *Comprehensive Materials Processing*, Elsevier, Amsterdam **2014**, p. 201.
[27] F. M. D'Heurle, J. M. E. Harper, *Thin Solid Films* **1989**, *171*, 81.

How to cite this article: P. Alizadeh, J. Franke, R. Dahlmann, *Plasma. Process. Polym.* **2024**, e2400018. https://doi.org/10.1002/ppap.202400018